Comparison of different droplet measurement techniques in the Braunschweig Icing Wind Tunnel

Inken Knop[1], Stephan Bansmer[1], Valerian Hahn[2,3], Christiane Voigt[2,3]

[1]Insitute of Fluid Mechanics, Technische Universität Braunschweig, 38108 Braunschweig, Germany

5 [2]Deutsches Zentrum für Luft- und Raumfahrt (DLR), Institute of Atmospheric Physics, 82234 Wessling, Germany

[3]Institute of Atmospheric Physics, University Mainz, 55881 Mainz, Germany

Correspondence to: Inken Knop (i.knop@tu-braunschweig.de)

Abstract. The generation, transport and characterisation of supercooled droplets in multiphase wind tunnel-test facilities is of great importance for conducting icing experiments and to better understand cloud microphysical processes such as coalescence,

10 ice nucleation, accretion and riming. To this end, a spray system has been developed, tested and calibrated in the Braunschweig Icing Wind Tunnel. Liquid droplets in the size range of 1 to 150 µm produced by pneumatic atomizers were accelerated to velocities between 10 and 40 m s^{-1} and supercooled to temperatures between 0 and -20 °C. Thereby, liquid water contents between 0.1 and 2.5 g m^{-3} were obtained in the test section. The wind tunnel conditions were stable and reproducible within 3% standard variation for median volumetric diameter (MVD) and 7% standard deviation for liquid water content (LWC).

15 Different instruments were integrated in the icing wind tunnel measuring the particle size distribution (PSD), MVD and LWC. Phase Doppler Interferometry (PDI), laser spectroscopy with a Fast Cloud Droplet Probe (FCDP) and shadowgraphy were systematically compared for present wind tunnel conditions. MVDs measured with the three instruments agreed within 15%, and showed high coefficients of determination (R²) of 0.985 for FCDP and 0.799 for shadowgraphy with respect to PDI data. The instruments' trends and biases for selected droplet conditions are discussed. LWCs determined from mass flow

20 calculations are compared to measurements of the bulk phase rotating cylinder technique (RCT) and the above single particle instruments. For RCT and PDI, agreement of approximately 20% in LWC was achieved, although in individual cases larger deviations depending on the flow conditions were detected. Using the different techniques, a comprehensive wind tunnel calibration for supercooled droplets was achieved, which is a prerequisite to provide well characterized liquid cloud conditions for icing tests for aerospace, wind turbines and power networks.

25 ## 1 Introduction

Supercooled water droplets cause icing of aircraft (Poots et al., 2000), helicopters (Kreeger et al., 2015), wind turbines (Battisti, 2015), and power networks (Farzaneh, 2008). As numerical icing codes are now widely used in the design and certification stages, the need for reliable experimental validation increases. The precise detection of the microphysical particle properties and the liquid water content (LWC) of droplet distributions produced by spray systems in wind tunnel test facilities thereby is

30 of great importance to improve ice accretion models. Besides icing research, other technical applications of spray systems,

such as fuel sprays (Bossard and Peck, 1996), agricultural sprays (Tuck et al., 1997), or spray painting (Snyder et al., 1989), are of interest for related industry and research.

Various measurement techniques that differ in terms of the underlying physical principles and the probe design are currently used to characterize droplet clouds. One way to classify these is the differentiation between integrating systems investigating the liquid clouds as a unity and single-particle instruments (Brenguier et al., 1998). Another possible criterion distinguishes between intrusive and non-intrusive systems (Tropea, 2011). Three types of measurement techniques allow to measure the total mass of an ensemble of liquid droplets: systems that calculate the LWC on the basis of single droplet size measurements (e.g., Fast Cloud Droplet Probe (FCDP), Phase Doppler Interferometry (PDI)), hot-wire methods (e.g., King LWC probe, Nevzorov probe), and ice accretion methods (e.g., rotating cylinder technique (RCT), icing blade) (Ide, 1999). A comprehensive overview of available techniques for cloud measurements is given by Baumgardner et al. (2017) including results from previous methodological papers (Tropea, 2011; Fansler and Parrish, 2015; Linne, 2013).

Here we show results from droplet measurements performed in the Braunschweig Icing Wind Tunnel (Bansmer et al., 2018) initially designed to offer large supercooled droplets (median volumetric diameter (MVD) ≈ 80µm) and ice particles for icing experiments in mixed phase and ice crystal conditions. In 2016 the wind tunnel has been further upgraded to introduce also small liquid droplets, relevant e.g. for research on wind turbine icing. During the extensive calibration of the new spray system different measurement techniques were integrated into the wind tunnel to measure the particle size distribution (PSD) and the LWC. Measurements of the PSD of liquid particle ensembles with droplet sizes < 200 µm were performed with the PDI, the FCDP and shadowgraphy and results are compared within the instrumental measurement ranges. In addition, the LWC detected with the PDI, the FCDP, and the RCT are compared and related to LWC calculations, based on injected water mass flow and wind tunnel flow velocity. Thereby the laboratory environment of the wind tunnel provides a homogenous ensemble of water droplets at a given constant target speed.

Similarly, to the experiments conducted here, Ide (1999) compared different LWC measurement techniques in the NASA Glenn Research Center Icing Tunnel. The instruments tested in 1999 were the icing blade, a single rotating cylinder, the Johnson-Williams and CSIRO-King hot-wire probes, the Nevzorov LWC/TWC (Total Water Content) probe, and the LWC calculated from the combined droplet distributions of two droplet sizing probes – the FSSP and the Optical Array Probe (OAP Particle Measuring Systems, Inc. Of Boulder, Colorado). Cober et al. (2001) published a comparison of different LWC measurement techniques for large supercooled droplets in flight tests. They evaluated a Rosemount icing detector from Goodrich Corporation, which can measure the LWC when boundary conditions lead to a temperature below the Ludlam limit. Furthermore, two FSSP and three different 2D-imaging systems (FSSP 100, 2D-C, 2D-P, all from PMS) were installed during their cloud research flights. Later on, the results of these publications are used for comparison purposes.

This paper describes the experimental setup of the Braunschweig Icing Wind Tunnel, the new designed spray system and its performance. After the description of the individual measurement techniques, results for MVD and LWC are discussed in sight

of the different measurement methods. The outlook presents a short summary, future research topics and plans for a second

65 update of the spray system to generate bimodal PSDs.

2 Experimental Setup

A detailed overview of the Braunschweig Icing Wind Tunnel is given by Bansmer et al. (2018). The basic design is a closed-loop wind tunnel with a 0.5 m x 0.5 m cross-sectional area at the test section with adjustable velocities between 10 and 40 m s^{-1}. The static air temperature can be controlled between -25 °C and +30 °C. In addition to the injection of water droplets through

70 a spray system, it is also possible to introduce a cloud of ice particles to simulate different conditions of atmospheric icing in the test section.

The spray system used here consists of 30 pulsed air-assist atomizers (see Fig. 1) from Spraying Systems Co (PulsaJet AB10000JJAU) with fluid cap PFJ-08-50 (diameter of the final liquid discharge orifice 0.2 mm) and air cap PAJ-73-1-60 (diameter of the final orifice outlet of 1.5 mm). The general random nature of the atomization process results in sprays with a

75 wide spectrum of droplet sizes with the mean value depending on the supply pressure (Lefebvre and McDonell, 2017). The electrically-actuated atomizers are controlled by the AutoJet Spray Controller. The pulse width modulated (PWM) flow control enables an independent change of liquid mass flow at constant supply pressure (and therefore relatively constant droplet size). The atomizers are switched on and off up to 10000 times a minute, making the spray appear constant for the purpose of icing research. Furthermore, the electrically-actuated spray nozzles are closed if not in use, even if the system is already pressurized.

80 This leads to a smaller delay from starting the spray to steady-state condition of the fully developed droplet size distribution. Demineralized water is used for droplet generation with a very low level of contamination to avoid clogging of the spray nozzles and freezing out of the droplets in the cold airflow. All components of the supply structure outside the tunnel were chosen with regard to small pressure losses and compatibility of materials for the demineralized water. Separate valves for every spray bar enable a selective usage of only a specific part of the atomizers. A separate management system to control

85 every atomizer individually has been implemented to turn off specific atomizers (e.g., in the case of low flow velocities and high probability of icing of the wind tunnel walls, the spray atomizers near the wind tunnel walls can be stopped). Thermal volume flowmeters measure the averaged water flow rate for each spray bar, thus providing a hint when nozzles clog or freeze over. The actuation of the electrically controlled pressure regulators for the water and the compressed air, all valves, and the control unit of the PWM-flow system are integrated into the wind tunnel software, providing the user with remote control of

90 the whole spray system. All aerothermal characteristics, like airflow uniformity, turbulence intensity, and total temperature of the wind tunnel flow, comply with SAE ARP5905 specifications (Bansmer et al., 2018).

The droplet measurements were conducted along the centerline in the wind tunnel test section 4 m downstream from the spray system. The bluff body shape of the spray bars (see Fig. 1) supports a homogenous spatial dispersion of droplets in the airflow. It has been shown numerically that droplets up to a diameter of 100 µm have almost no slip to the wind tunnel speed (Bansmer

95 et al., 2018), leading to the assumption that the droplet velocity in the test section agrees well with the adjusted air speed. The

temperature and airspeed of the flow can be regulated with the required accuracy according to ARP5909, however, the humidity and static pressure cannot. The static pressure in the test section is hence dependent on the ambient pressure, whereas the humidity in the test section is governed by the duration of water injection. Shadowgraphy, PDI, and FCDP measurements of droplet PSDs and LWC were performed in test campaigns in 2017 and some PDI measurements were repeated in 2019. The

100 static pressure in the test section varied during these measurements between 990 hPa and 1007 hPa. Most of the experiments were conducted at temperatures between -10 °C and 0 °C to avoid fogging of the wind tunnel windows and instrument optics. The relative humidity of the two-phase flow quickly increased after the first few tests at the beginning of a measurement day to > 90%. For a better description of the temporal stability of the wind tunnel and spray system boundary conditions, Fig. 2 shows a representative 15-minute test record. The upper three diagrams describe the quality of the wind tunnel flow and the

105 lower three diagrams the spray system. All measured flow quality parameters meet the requirements of the ARP5909 for the temporal stability in the tunnel centreline and thereby the measurement positions of the intercomparison tests: The flow velocity fluctuates by a maximum of 1.6%. The tunnel temperature varies by less than 0.5 °C and the relative humidity, as the only non-adjustable variable, varies by max. 1.5% over a time period of 15 minutes.

The air and water pressures in the supply system of the spray nozzles fluctuate by max. 0.1 bar. These constant supply system

110 parameters are a prerequisite for a temporally constant atomisation process and thus a temporally constant droplet cloud in the test section. By monitoring the water mass flow, it can be determined that, despite previous pressurization of the pipes, approx. 15 seconds are required until the volume flow stabilizes. The later fluctuations in the volume flow are due to the unsteadiness of the atomization process itself and the mentioned uncertainty of the thermal volume flowmeters for small unsteady mass flows. According to the assumption that all droplets are accelerated with the airflow in the long wind tunnel nozzle, the

115 downstream position of the measurement volume in the test section should neither significantly affect the droplet diameter nor the droplet velocity or LWC. Depending on the mechanically required window configuration of the test section for every measurement setup, the downstream coordinate of the probe volume differed slightly. The measurement position of the PDI (or the RCT) and the shadowgraphy (or the FCDP) varied by a maximum of 220 mm (see Fig. 3) in downstream position.

Procedures for determining appropriate sample size, size class widths, and characteristic droplet sizes for the characterization

120 of sprays were applied according to ASTM E799-03 (Practice for Determining Data Criteria and Processing for Liquid Drop Size Analysis). In icing research, the histogram of the number of droplets with diameters between D ± ΔD/2 is used most frequently, together with cumulative curves of the liquid cloud volume. In this study, the characteristic diameters of the cumulative volume curve like the MVD (or DV0.5) and the 10 and 90 percentiles (DV0.1 and DV0.9) are used to describe the droplet distributions as shown in Fig. 4 for a test delivering a cloud ensemble with an MVD of 11.6 µm. Droplet distributions

125 in the atmosphere typically follow a log-normal behaviour (Langmuir and Blodgett, 1961). The atomization of fluids in laboratory setups may lead to different particle size distributions such as normal, Nukiyama–Tanasawa, Rosin–Rammler, modified Rosin-Rammler, and upper-limit distributions (Lefebvre and McDonell, 2017). Here, we indicate the distributions and their fits in the respective experiment.

Another important variable for icing research is the already mentioned LWC, which represents the mixing of the available
mass of water within a defined air volume:

$$LWC = \frac{m_{Water}}{V_{air}} \qquad (1)$$

The repeatability of measurements is characterized based on the coefficient of variation (i.e., the standard deviations over
several repeated measurements normalized by the mean values):

$$\sigma = \frac{1}{\overline{MVD}} \sqrt{\frac{\sum(MVD - \overline{MVD})^2}{n}} \qquad (2)$$

To describe the consistency of the results from different measurement techniques, we use the mean absolute value of the
relative error. Therefore, the sum over all differences in the value of interest between the considered and the reference
technique, normalized by the reference value, is divided by the number of comparable measurements. The absolute value of
the difference avoids a cancellation of positive and negative errors.

$$|E_{MVD}| = \frac{1}{n} \sum \frac{|MVD_{compare} - MVD_{PDI}|}{MVD_{PDI}} \qquad (3)$$

For the evaluation of the deviations between the different measuring techniques, an investigation of the repeatability of the
droplet cloud in the wind tunnel is needed. Due to the afore mentioned small pressure fluctuations in the supply system and
slight fluctuations in the wind tunnel velocity, minor variations in the droplet size distribution and the LWC may occur even
with the same settings for all wind tunnel parameters. In addition, there is the non-deterministic atomization process at the
pneumatic atomizers themselves (Liu et al., 2005) leading to small temporal variations in the droplet cloud. To determine the
size of these variations for the MVD in the Braunschweig Icing Wind Tunnel reference measurements have been performed
with the PDI and selected measurement points have been repeated with exactly the same experimental setup. The results of
some of these tests are shown in Fig. 5. The repeatability of MVD and the corresponding PSD is within ± 3% standard
variation. For the same test points, the LWC based on the water mass flow was also investigated. This resulted in a standard
deviation of the LWC in repeated measurements of 7%, indicating altogether a good repeatability of the wind tunnel conditions
with respect to particle size and LWC.

In a typical droplet size distribution in a spray in the wind tunnel, large droplets occur by orders of magnitude less frequent
than small droplets (Rudoff et al., 1993; McDonell and Samuelsen, 1996). Therefore, the choice of the number of droplets per
test point is essential for a representative and comparable determination of the MVD. To determine the desired number of
droplets for a test point, one exemplary test point was measured over 15 minutes with the PDI system at constant boundary
conditions. Figure 6 shows the dependence of the MVD on the number of droplets taken into account. Since the MVD is
sensitive to large droplets, its stability is a good hint for a representative measurement point. Taking into account more than
10000 droplets for the test point results in less than 5% deviation from the mean value over 280000 droplets. This minimum
number of droplets was set as a target value for all experiments.

The test matrix for the measurements was designed to test each independent variable separately. To this end, the droplet
diameters were first varied using different combinations of air and water pressure. During these tests the duty cycle of the

nozzles and the velocity and temperature of the tunnel were not changed. Then, the duty cycle was varied for selected pressure combinations in order to classify its influence on the MVD and LWC. Furthermore, the flow velocity was changed from 20 to 30 to 40 m s^{-1} with exactly the same spray system settings, which should lead only to changes in LWC. Finally, the temperature was varied, which theoretically should neither have a noticeable influence on the droplet size nor the LWC. In addition, the parameters of every measurement technique were varied depending on the individual system.

3 Measurement Techniques to determine PSD and LWC

Figure 3 shows an overview of the different measurement setups in the Braunschweig Icing Wind Tunnel. The following sections present the measurement instruments, their parametrization, as well as their inherent advantages and shortcomings. When using optical methods, particular attention must be paid to the correct description and interpretation of the sample area, the cross-sectional area perpendicular to the flow velocity where droplets are detected. The sample area is defined by the optical and electronic configuration of the instrument (Widmann et al., 2001).

3.1 Phase Doppler Interferometry

The Phase Doppler Interferometry (PDI) is a single-particle counter, single point, real-time, and non-intrusive measurement technique and an extension of the Laser Doppler Anemometry (LDA), initially described in 1972 by Farmer (Farmer, 1972). Since the early 1980s, i.a. Bachalo has further advanced the principle into the PDI (Bachalo and Houser, 1984). The basic principle of LDA and PDI is based on the detection of the characteristic refraction signal of a spherical particle passing through an interference fringe pattern created by two coherent intersecting laser beams. The velocity of the particle (LDA) can be determined via the Doppler difference frequency of the scattered light signal. In the PDI system, the receiver lens is additionally spatially partitioned into several segments. The spatial phase shift between the different detectors contains the size information of the particle (Durst and Zaré, 1975; Bachalo and Houser, 1984; Cossali and Hardalupas, 1992). The PDI theoretically only needs an initial factory calibration because the parameters responsible for the measurement results, like the laser wavelength, beam intersection angle, transmitter and receiver focal lengths, do not change within the lifetime of the system.

The PDI system used in this investigation is the 2D modular PDI from Artium Technologies Inc. It consists of an optical transmitter (diode-pumped solid-state laser), an optical receiver, Fourier-transform-based advanced signal analyzer (signal processors), a data management computer, and the AIMS system software. The PDI has been used within two different setups that are described with their characteristic numbers in Table 1.

The photomultiplier tube (PMT) voltages were chosen carefully with regard to the expected diameter distribution and volume flux. Several early investigations of the PDI system have shown the effect of the PMT gain on the measurements (Bachalo et al., 1988; McDonell and Samuelsen, 1996). The signal processor was operated with the settings chosen by the manufacturer's automatic setup. The investigation of the sensitivity of the PDI setup to user-controlled settings of McDonell and Samuelsen (1990) showed variations in the MVD of 5%. A later study by McDonell et al. (1994) found a mean coefficient of variation in

D$_{32}$ of 10%. The higher variability in the second study can be explained according to Lefebvre and McDonell (2017) by different lab conditions and user behaviour.

In the evaluation of the PDI results for size distribution and LWC, the probe volume correction (PVC) described inter alia in Zhu et al. (1992) was considered for all measurements. This correction is based on the assumption that smaller particles passing a Gaussian-shaped probe volume have only a smaller area where they can be detected because of their lower scattering intensity (scattering light can be taken as being proportional to the square of the droplet diameter (McDonell and Samuelsen, 1996)). Small particles need to pass the maximum intensity in the centre of the probe volume to produce scattering signals high enough to be detectable. Larger droplets can still be detected when they pass at the edge of the Gaussian-shaped probe volume. Using the transit time method (Zhu, 1993), the real probe volume for every size class is measured independently and used for correction of the size distribution afterwards.

The calculation of the LWC from the PDI measurements is based on the corrected volume mean diameter D$_{30}$ and the corrected droplet number concentration N$_d$, with the following formula (Widmann et al., 2001):

$$LWC = \frac{\pi}{6}\rho D_{30}^3 N_d \tag{4}$$

The corrected volume mean diameter of the size distribution D$_{30}$ is calculated with the probe volume corrected counts per size bin.

$$D_{30} = \sqrt[3]{\frac{\sum_{i=1}^n c_i^{cor} d_i^3}{\sum_{i=1}^n c_i^{cor}}} \tag{5}$$

$$c_i^{cor} = c_i \left(\frac{V_{max}}{V_i}\right)\left(\frac{D(d_i)_{max}}{D(d_{max})_{max}}\right) \tag{6}$$

The probe volume corrected counts c_i^{cor} are related to the effective probe volume per size class V_i, determined by the afore mentioned transit time method. For the calculation of the corrected droplet number concentration N$_d$, the ratio of the total particle transit time $t_{tran(i,j)}$ and the total sample time t_{Tot} is divided by the probe volume PV_i for each particle size class.

$$N_d = \frac{1}{t_{Tot}}\sum_i \frac{\sum_j t_{tran(i,j)}}{PV_i} \tag{7}$$

The PVC has the greatest effect on the smallest size classes. Their influence on the LWC, on the other hand, is very small. In addition to the PVC, an intensity validation scheme, described by Bachalo (2000), was used. This procedure supplements the PDI principle with a validity check, in which the agreement between signal intensity and droplet diameter calculated from the burst distance is checked. Overall, the approach to determine the LWC from the droplet size distribution increase the measurement uncertainties compared to direct LWC measurement methods (Lance et al., 2010), which has been shown e.g. by McDonell et al. (1994) and Widmann et al. (2001). McDonell et al. (1994) find variations in droplet concentration of up to 50%. Widmann et al. (2001) investigated the accuracy of LWC measurements from the PDI in an application with only low data rates and find a coefficient of variation of up to 38%. From these measurements it can be followed that the droplet concentration is generally very sensitive to instrument operation and chosen settings. Because of the high number of influencing parameters, it is not surprising to see large variations in the results of re-runs (McDonell et al., 1994; Tropea,

2011). According to Bachalo et al. (1988) and Zhu et al. (1992), the calculation of the correct probe area is the primary source of error in the calculation of the volume flux.

3.2 Fast Cloud Droplet Probe

The Fast Cloud Droplet Probe (FCDP) manufactured by SPEC Inc. is a single particle counter, which uses forward scattering of light by particles passing through a laser beam to derive the particle size and concentration. Hence FCDPs are often used to detect microphysical properties of liquid clouds from research aircraft (Lawson et al., 2017; Woods et al., 2017; Voigt et al., 2017; Taylor et al., 2019).

The particle size is determined via the correlation between the scattering cross-section under the assumption of Mie-theory and the signal voltage measured at the signal detector. A qualifying detector confines a focal area along the laser beam. This Sampling Area (SA) is composed of the Depth of Field (DoF) along the Laser beam and the Effective Beam Diameter (EBD) perpendicular to the incident flow and DoF. The detected particles are resolved into 21 size bins ranging from 1.5 µm up to 50 µm. Some of the spray properties that can be derived from the measurements are the droplet number concentration N_d, MWD and LWC. The operation principle of the instrument, as well as sources of uncertainties are described in detail by Lance et al. (2010), Baumgardner et al. (2017), Lawson et al. (2017) and Faber et al. (2018).

Lance et al. (2010) report an accuracy in particle sizing of the recalibrated CDP not to be better than 10% (mainly due to the coarse size resolution of the size bins). Baumgardner et al. (2017), on the other hand, report up to 50% uncertainty in sizing for single-particle scattering probes like the FCDP. In experiments with a monodisperse droplet generator, Faber et al. (2018) detect a sizing error of less than 10%, depending on droplet size and transit location across the sample area.

For the LWC, Baumgardner (1983) estimates an accuracy of 32-34% for results from droplet scattering methods. Lance et al. (2010) show on the basis of laboratory calibrations with water droplets and Monte Carlo simulations that the CDP accurately measures droplet number concentrations up to 200 cm^{-3}. The detection of higher number concentrations may experience relatively large under- or overcounting effects. Also oversizing errors due to coincidence result in larger errors in higher-order products, such as the LWC (Lance et al. (2010).

Unlike the PDI system used here, the FCDP was installed inside the wind tunnel with the measurement volume placed in the undisturbed particle-laden flow at the centre of the test section. Table 2 gives an overview of the main characteristics of the probe. For the calculation of N_d, the true airspeed (TAS) from the wind tunnel was used as droplet velocity. The FCDP used in this study has novel fast electronics, which partially minimizes coincidence effects by calculating coincidence correction functions based on transit time information and other data stored with each individual particle. After confining the sampling area to a reasonable size relative to the measured droplet number concentration, the correction discards all droplets with a beam transit time larger than 125% of the theoretically calculated value for this droplet size at a given true air speed (Lawson et al., 2017; Woods et al., 2017; Thornberry et al., 2017) and allows to measure particle concentrations up to >1000 cm^{-3} within the experimental uncertainties. High particle number concentrations as in some conditions produced by the wind tunnel facility can be encountered in the atmosphere in polluted low clouds (Flammant et al., 2018; Taylor et al., 2019), polluted convection

(e.g. Braga et al., 2017b; Ceccini et al., 2017) or in young contrails (e.g. Voigt et al., 2011; Kaufmann et al., 2014; Kleine et al., 2018).

In total, more than 80 different spray conditions have been measured each for about 120 s. For droplet distributions at low velocities, high temperatures, and with a significant number of droplets outside the certified measuring range of 50µm, the variation in MVD derived from FCDP measurements increases compared to the reference instrument.

3.3 Direct Imaging: Shadowgraphy

The idea of the shadowgraphy technique is to capture a shadow image of a particle. The system consists of a pulsed laser backlight and a diffuser which illuminates the particles passing the system between the light source and camera. The camera is equipped with a far-field microscope and magnification lenses. The double-pulsed laser allows for the recording of short-time-separated pictures and therefore additionally the calculation of droplet velocities with particle tracking algorithms. Like the PDI, the shadowgraphy technique is also counting single particles without influencing the flow. For the correct interpretation of the measurement images, a prior calibration is necessary. The range in which droplets can be detected and correctly sized is limited by the image area of the camera chip and by the depth of field of the optical system. Finally, the shadow pictures are post-processed with an image analysis software (DaVis from LaVision), which determines the diameters of the shadow images in the field of view.

A border correction filter and a depth of field correction according to Kim and Kim (1994) were applied in the post-processing step. Since the image rate of the camera and laser assembly is limited, a long measurement time is required for a statistically robust result. The detailed post-treatment of shadow images has been described by Kapulla et al. (2007) and Kapulla et al. (2006). According to Baumgardner et al. (2017) imaging techniques can suffer from uncertainties up to 100% in size measurements. The evaluation of the shadowgraphy pictures is rather focused on the size distribution and not on the LWC because of high uncertainties in the probe volume and consequently the droplet number concentration. The hardware settings used in the experiment conducted here are listed in Table 3. Because of the long measurement time for every test point (10 - 20 min), only 40 measurements in total were conducted. Among these 40 measuring points, there are many repeated measurements and measuring points with varied tunnel velocity but the same spray settings, leading to almost identical droplet size distributions in the evaluation.

3.4 Rotating Cylinder Technique

According to the SAE International Standard ARP5905 (Calibration and Acceptance of Icing Wind Tunnels), a rotating cylinder based on Stallabrass (1987) was designed and constructed for the Braunschweig Icing Wind Tunnel. The rotation of the cylinder ensures a uniform ice build-up around the circular cross-section that provides aerodynamic consistency while accreting ice. If the speed of droplets, cylinder geometry, ice density, and collection efficiency (known droplet diameter) are known, the LWC can be calculated by the following formula:

$$LWC = \frac{\pi \cdot \rho_e}{\alpha_1 \cdot u_\infty \cdot t} \cdot \left[\left(\frac{m_e}{\pi \cdot \rho_e \cdot l_c} + r_c^2 \right)^{0,5} - r_c \right],$$ (8)

where ρ_e (assumed to be 880 kg m⁻³) stands for the ice density, m_e for the final accreted ice mass, t for the icing time (selected with regard to the maximum allowed ice accumulation), α_1 for the collection efficiency, and l_c and r_c for the length and the radius of the original cylinder, respectively. The calculation of the collection efficiency is based on the assumption of a monodisperse droplet distribution with the MVD as the diameter for all droplets.

In this measurement method, several assumptions that lead to uncertainties in the LWC results are made. These are based on the SAE ARP5905 uncertainties in bulk density of ice, the simplification of the droplet size distribution to one representative diameter (MVD) and the assumption of a fixed cylinder diameter in the calculation of collection efficiency.

With the density of accreted ice depending on several parameters (temperature, droplet velocity, etc. (Macklin, 1962; Jones, 1990)), a 12.5% error in the assumed bulk density of ice leads to 3% error in LWC, according to Stallabrass (1978). The simplification to regard the entire droplet cloud as a monodisperse spray with only droplets of the diameter of the MVD enters the calculation of the collection efficiency. Early investigations have shown that, for example, the assumption of a monodisperse droplet size distribution instead of a Langmuir D distribution of the droplet size leads to an overestimation of the collection efficiency of 3.5% at 25 m s⁻¹ and MVD = 20 µm (Langmuir and Blodgett, 1946). According to SAE ARP5905, the average diameter between non-iced and maximum iced cylinders for the calculation of the collection efficiency leads to an error of 1-2% in collection efficiency.

Two rotating cylinders were used for this testing with 2.5 mm (according to ARP5950) and 5 mm (for comparison) in diameter. The cylinders were rotated at 60 rpm. At the beginning of every run, the cylinder was shielded until the conditions had stabilized (approximately 15 s). All tests were performed at temperatures of - 18 °C or below to create rime ice, which is an essential requirement for this method (Ludlam, 1951). Differing from the previously mentioned systems, the RCT is an integrating and intrusive system. In this application, the MVD was taken from the PDI measurements and the LWC was measured by the RCT. In total, nearly 100 test points were investigated.

3.5 LWC based on Water Flow Rate and Wind Tunnel Speed

The LWC in the icing wind tunnel can be determined from the total injected water mass flow and the circulating air volume flow. There are two prerequisites for the application of this procedure:

1) there is no recirculating water;

2) there is a known moist air volume flow (depending on flow velocity and droplet size).

The first assumption is true for an air temperature below 0 °C. In these conditions, the droplets will supercool and freeze out by hitting a surface of the wind tunnel, e.g. turning vanes of the first or second corner, collecting grid, fan or heat exchanger. To determine the moistened air volume flow in the wind tunnel, several icing tests on a grid were performed. The area over which the droplets spread depends on the wind tunnel speed and the droplet size or the air pressure used at the spray nozzles for droplet generation. Several tests were performed to measure the 2D-iced area in the test section and to estimate the LWC

in the borders close to the wind tunnel walls. On the basis of these assumptions, the LWC can be calculated with the following

320 formula:

$$LWC = \frac{\dot{m}_{Water}}{\dot{V}_{Air}} = \frac{\dot{m}_{Water}}{\alpha \cdot A_{testsection} \cdot u_{\propto}}, \tag{9}$$

where $\dot{m}_{Water}$ is the injected water mass flow, α is the percentage of the moistened cross-sectional area, $A_{testsection}$ the cross-sectional area, and $u_{\propto}$ the tunnel velocity. These numbers are available for all measurements and take also into account the clogging of nozzles during the experiment. Thereby, this method offers a good reference for LWC comparison.

4 Experimental Results and Discussion

325

The results of the intercomparison of the different measurement techniques are presented in this section. Tropea (2011) identifies three main sources of error in the measurement of size distributions with optical techniques, liquid fluxes, and droplet number concentration, which are inherent in all optical measurements conducted here: errors in droplet sizing, errors in counting (missed particles, coincidence) and errors in the sampling area (or volume) estimation.

330 The measurement uncertainties in droplet number concentration and sizing result in greater uncertainties for higher-order products such as LWC calculated from the observed cloud droplet size distributions. Overall, according to Tropea (2011), the uncertainty of mass flux measurements ranges from 20% up to several hundred percent. The results obtained here and described in the following have to be regarded in this context.

4.1 Repeatability of the Wind Tunnel Conditions and Accuracy of the Measurement Setups

335 The particular advantage of the comparison of measurement techniques in the conditions provided by the wind tunnel compared to measurements in clouds or at a single spray nozzle lies in the temporal consistency of the PSD in the centreline of the test section and the repeatability of the test conditions over several runs as shown in section 3 (3% standard deviation in repeated MVD measurements with the PDI and 7% standard deviation in the repeated LWC measurements based on the injected water mass flow). In order to evaluate the results of the intercomparison measurements of MVD and LWC, the

340 coefficients of variation of each measurement techniques are explained below. They are summarized in Table 4.

With the PDI system in addition to a variety of wind tunnel spray conditions, variations of the instrument setting such as PMT gain, sampling rate or the application of analogue filters have been tested. The overall combined repeatability of the wind tunnel conditions and the accuracy of the PDI setup resulted in a mean coefficient of variation of the MVD of $\sigma = 5\%$. DV0.1 and DV0.9 behave in a similar way, with an average coefficient of variation of $\sigma = 7\%$. In the context of the above mentioned

345 measurements (see Section 4.1), the coefficient of variation determined here indicates an adequate design of the PDI system and the correct choice of system parameters. However, the average of the coefficient of variation over all repeatability measurements in DV0.99 is slightly greater ($\sigma = 14\%$). The larger variation in DV0.99 is quite plausible since the very small proportion of large droplets can be detected statistically less frequently (see Fig. 7) but has a large impact on DV0.99

(McDonell et al., 1994). For this reason, their detection is affected by larger fluctuations even in measurements with a high

350   number of total measured droplets. The LWC results show considerably more variability. The measured average coefficient

of variation of about $\sigma = 20\%$ is four times greater than the variations in the MVD measurements but rather small if compared

to McDonell et al. (1994), Widmann et al. (2001) and Tropea (2011). According to Equation 4 the LWC calculation of the

PDI is proportional to the droplet number concentration N_d and to the third power of the corrected volume mean diameter D_{30}.

The present coefficients of variation of the representative droplet diameters thus can lead directly to 15-21% variation in the

355   LWC. Adding the uncertainty of the droplet number concentration the average coefficient of variation of 20% is coherent and

comparatively small.

The repeatability of the wind tunnel conditions together with the accuracy of the measurement setup has also been investigated

for the FCDP. On average, a coefficient of variation of $\sigma = 7\%$ in MVD was found for all repetition measurements. Similar

values were found for DV0.1 and DV0.9. Due to the large width of the size intervals (bins) of the FCDP for large particles,

360   the determination of DV0.99 on the basis of the FCDP data was not further evaluated. Taking into account the accuracies of

the FCDP for monodispersed single droplets, as mentioned in Section 4.2, the here found coefficients of variation of the

representative droplet diameters indicate a good repeatability of the new spray system of the Braunschweig Icing Wind Tunnel.

Like the PDI results, the LWC calculations from the FCDP also show a significantly higher coefficient of variation ($\sigma = 17\%$),

inherent in the method of deriving the LWC from measurements of the particle's size, see Baumgardner (1983) and Tropea

365   (2011).

The combined influence of the accuracy of the shadowgraphy setup and the wind tunnel repeatability leads to an average

variation of $\sigma = 8\%$ for the MVD, which is within the same order of magnitude compared to the afore-mentioned methods.

According to Lefebvre and McDonell (2017), the imaging system developed by the Parker-Hannifin Corporation has a

repeatability of 6% in the Sauter mean diameter range from 80 µm to 200 µm. Considering the significantly smaller droplets

370   sizes here, the slightly higher coefficient of variation is plausible, as small droplets represent the more challenging task for

direct imaging systems. Thus the here measured variations indicate a well-chosen measurement setup and data post processing

for the shadowgraphy technique.

The performed repeatability tests with the RCT lead to a coefficient of variation of $\sigma < 10\%$. Overall, SAE ARP5905 indicates

because of the mentioned sources of errors (see Section 3.4) a method accuracy of $> 90\%$, which can be verified by the

375   repetition measurements carried out in this study.

The overall accuracy of the mass-flow-based-calculation of the LWC is primarily limited by the accuracy in the measurement

of the water mass flow and the uncertainty in the determination of the moistened cross-sectional area. The water volume flow

is measured with one thermal volumetric flow meter per row of six atomizers. Due to the very low total water volume flow

through every thermal volumetric flow meter (down to less than 10 ml min⁻¹ per row) and the pulsation of the nozzles, the

380   uncertainty of the volume flow measurement is approximately 20%. The mean coefficient of variation of repeated test cases

for the calculated LWC over the water mass flow and the moistened air volume is $\sigma = 7\%$.

4.2 Comparison of MVD measurements from the different instruments

A common well characterized technique to measure spherical droplets in technical sprays is the PDI, see Basu et al. (2018), Kapulla et al. (2007) and Jackson and Samuelsen (1987). Here, the PDI is also used as a reference instrument for the MVD

385 due to its long heritage of measurements in the Braunschweig Icing Wind Tunnel including all measurement conditions for the intercomparison. The FCDP and the shadowgraphy data are compared to the PDI results in the following analysis. Figure 8 shows an overview of the MVD measurements from all techniques with the coefficients of variations explained above, indicated as error bars.

To compare FCDP and PDI results, the range of the PDI data evaluated for the intercomparison was limited to a maximum

390 droplet diameter of 50 µm in a post-processing step to match the upper particle size limit of the FCDP.

Generally the MVDs derived from the PDI and the FCDP agree within 14% for droplets generated in the size range between 5 and 50 µm. The linear best fit ($\text{MVD}_{\text{FCDP}}=0.91\cdot\text{MVD}_{\text{PDI}}$) through the data points has a coefficient of determination of $R^2=0.9853$. The mean absolute value of the relative difference between the FCDP and the PDI measurements is $|E_{\text{FCDP - PDI}}| = 7.7\% \pm 3.9\%$. When comparing the relative deviations of the two instruments, for PSDs with MVDs $< 20\,\mu m$

395 the agreement between PDI and FCDP is nearly 100% and for distributions with MVDs $> 20\,\mu m$ the FCDP measures on average 9% lower MVDs compared to the PDI (see Fig. 9 left). A low sensitivity of the FCDP to larger particle sizes ($> 30\,\mu m$) may cause or contribute to the measured deviation of the FCDP with respect to the PDI for large droplets. This deviation for larger MVDs might also be explained by a slight velocity deficit between large droplets and the airflow, which can be seen in the PDI measurements (see Fig. 10 for an exemplary velocity distribution for the marked measurement point in Fig. 9). The

400 transit time filter applied to the FCDP data during post-processing to reduce coincidence causes a rejection of droplets that have a too long transit time compared to the mean reverence velocity and thus reduces the droplet size spectrum evaluated as valid by large droplets.

The coincidence correction for high particle concentrations (Lance et al., 2012; Lance et al., 2017) (right side of Fig. 9) cannot explain the observed low bias of the FCDP for large particle sizes. In contrast, the lowest deviation in MVDs is detected at the

405 higher particle concentrations up to 2000 cm^{-3}. Taking into account the above mentioned coefficients of variations for both measurement setups and the repeatability of the wind tunnel the overall agreement is very good.

According to Lance et al. (2010), an additional source of error of the CDP might be the external geometry of the probe, which can alter the measured cloud particle size distribution. The shattering of large droplets and ice crystals, either by direct impaction with the instrument arms extending upstream of the sample volume or by the shear forces as the particles are

410 deflected by the airstream flowing around the probe, can influence the results (McFarquhar et al., 2007; Weigel et al., 2017). This effect can have a minor influence on the measurements in the wind tunnel test section at TU Braunschweig since the probe is an intrusive instrument while the other particle counters were mounted outside of the test section (see Fig. 3). Ice accretion on the non-heated parts of the probe might additionally alter the local two-phase flow in the upstream direction (see Fig. 3).

415   In general the here found agreement in MVD between FCDP and PDI with 14% is well within the range of previous instruments intercomparisons (Faber et al., 2018; Braga et al., 2017).

To ensure measurement mutual size ranges between the PDI and the shadowgraphy system the minimum diameter of the PDI results was corrected to 10 µm in post-processing. The results of the shadowgraphy measurements are depicted in Fig. 8 as diamonds. Larger variations were detected by shadowgraphy for particle sizes larger than 35 µm.

420   The linear best fit ($MVD_{Shadowgraphy}=0.97 \cdot MVD_{PDI}$) through the data points with a $MVD < 35$ µm has a coefficient of determination of $R^2=0.7985$ and is therefore smaller than the one from the FCDP data. The mean absolute value of the relative difference between the FCDP and the PDI measurements is $|E_{FCDP - PDI}| = 9.9\% \pm 6.3\%$. The eight measurement points with higher $MVDs_{PDI}$ have not been taken into account for the best fit curve since they differ greatly from the PDI results. A possible explanation for these measuring points with significantly smaller MVD can be found in the typical drop size distribution: the

425   percentage of large droplets is very low in our typical wind tunnel diameter distributions (see Fig. 7). Rudoff et al. (1993) showed also in NASA's Glenn Research Center's Icing Research Tunnel (IRT) that the droplet distribution can have a long tail towards large droplets, which can only be detected reliably with very long measurement durations. With the shadowgraphy setup used here, only very low data rates could be measured. As a result, often only 3000-6000 droplets per spray condition were measured despite long test times (> 15 min). With the DOF and border correction, this leads to an average of more than

430   20000 droplets per distribution. Large droplets, however, are added only slightly (through the border correction) or not at all. It is therefore thinkable that, due to their rare statistical occurrence, no large droplets were detected in the originally measured droplet size distributions, eventually leading to an incorrect representation of the MVD. The overall agreement between shadowgraphy and PDI results matches previous measurements, e.g. Kapulla et al. (2007) and Rydblom et al. (2019).

4.3 Comparison of LWC measurements from the different instruments

435   Figure 11 shows the measurement results of the PDI, the FCDP, and the RCT compared to the LWC calculated from the injected water mass flow. Often bulk phase instruments such as the rotating cylinder or a hotwire are used for the determination of the LWC. In some cases it might be an option to derive the LWC from the measured PSD (measured e.g. with the PDI or the FCDP) with some inherent uncertainty in this method, including the third order dependence of the LWC on the particle diameter. As expected, the comparison shows a significantly greater degree of variation compared to the droplet size results,

440   which is discussed in more detail in the following.

The mean absolute value of the relative difference between the PDI results and the LWC calculation based on the water flow rate is $|E_{PDI - WFR}| = 24\% \pm 32\%$. Despite the large absolute value of relative difference, the mean best fit line ($LWC_{PDI} = 0.9 \cdot LWC_{WFR}$ with coefficient of determination of $R^2=0.7020$) fits well to the results of the water mass flow method. From over 130 data points with $LWC_{WFR} < 0.5$ g m⁻³, more than 90% from the PDI results fall within a range of ± 0.1 g m⁻³

445   around the LWC_{WFR} (86% of $LWC_{WFR} < 0.3$ g m⁻³ in the range ± 0.05 g m⁻³). Chuang et al. (2008) performed an intercomparison of the airborne PDI to a Gerber Scientific Inc. PVM-100A (a probe based on forward light scattering (Gerber et al., 1994)) and obtained a good consistency for LWC of up to 0.3 g m⁻³ with an accuracy of ± 0.05 g m⁻³ containing 85% of

data points, which, despite the different velocities, is in good agreement with the results obtained here. Of the more than 150 remaining measurement results of the PDI with an LWC > 0.5 g m⁻³, only 56% lie within a range of ± 20% around the LWC

450   calculated from the water mass flow. In situ measurements by Cober et al. (2001) in supercooled large droplet conditions compared the integrated LWC from the droplet distribution of FSSP and 2D-C and 2D-P to the results of the Nevzorov probe. A slightly higher LWC result from the integrating systems was found compared to the Nevzorov probe. 90% of the measurement points with an LWC > 0.1 g m⁻³ fall into the 1:1 correlation with ± 43%. In our experiments, 91% of all PDI results with an LWC > 0.1 g m⁻³ fall into the 1:1 correlation with ± 43%. Therefore, our results, which partly also contain

455   droplets > 100 µm, are comparable to the results of the flight tests of Cober et al. (2001).

For a detailed analysis of the LWC results of the PDI, Fig. 12 shows the ratio of LWC_{PDI} to LWC_{WFR} over the MVD measured by the PDI and over the air velocity in the wind tunnel. Plotting the LWC over the MVD indicates a small tendency to underestimate the LWC with the PDI with increasing MVD (>35 µm). Plotting the LWC ratio against the wind tunnel velocity it can be seen that at low velocities the PDI results are above the LWC calculated over the mass flow and with increasing

460   velocities the LWC_{PDI} tends to become lower than the reference values. A similar result was obtained by Rudoff et al. (1993) for the IRT. To see whether this dependency can be attributed more to the wind tunnel and the water mass flow methodology or the PDI, the other measurement techniques are first examined in detail.

If also assuming an uncertainty of ± 20% for the PDI results, more than 90% of the LWC measurement data overlap between the PDI and water mass flow. The comparison of the measurement results supports the already mentioned greater uncertainty

465   in the LWC measurements.

The results of the FCDP show a larger variation with respect to the reference. The linear best fit $LWC_{FCDP} = 1.12 \cdot LWC_{WFR}$ has a coefficient of determination of R²=0.3276. Overall there is a systematic high bias of the LWC derived from the FCDP compared to the PDI, despite eventually smaller particles sizes detected by the FCDP. This can only be explained by higher particle number concentrations measured by the FCDP compared to the PDI. An overestimation of the LWC by the use of

470   scattering spectrometers has been found previously in comparative experiments (Rydblom et al., 2019; Faber et al., 2018; Ide, 1999). For the FSSP forward scattering probe, Baumgardner (1983) found 20-200% higher LWC values than measured by hot-wire probes. In the measurements by Ide (1999), the LWC calculated from the droplet diameter distributions overestimated the LWC for MVDs up to 50 µm by 50% and even up to 100% and 150% for higher MVDs. Faber et al. (2018) have suggested the velocity difference between his laboratory measurements and aircraft measurements, for which the CDP is originally

475   designed, as a possible reason for the large overestimation of LWC. This could also be a possible explanation for the results obtained here. To examine the results in detail, Fig. 13 shows the ratio of LWC_{FCDP} to LWC_{PDI} versus MVD_{FCDP} and versus $N_{d\ FCDP}$.

Unlike the PDI, a correlation between the FCDP data for LWC and droplet size seems to be obvious. Measurements with an MVD > 27 µm are the only ones leading to an underestimated LWC. These measurement points also correspond to the data

480   points with low data rates and low particle concentrations (see the right section of Fig. 13). Due to the limited size range of the FCDP and the broad width of the size bins, the underestimation of the LWC can be caused by some of the droplets present

in the flow but not visible for the FCDP and droplets erroneously sorted out as coincidental particles. At high N_d and small droplet diameters, the FCDP significantly overestimates the LWC. The dependence of LWC on droplet concentration was also reported by Lance et al. (2010), albeit in inverse form. Higher droplet number concentration exhibit higher coincidence effects and lead to an overestimation of the particle size. However Fig. 8 clearly shows an agreement of 7% within the probes and eventually a low bias of the MVD detected with the FCDP.

The results of the RCT are illustrated by black diamonds in Fig. 11. The mean absolute value of the relative difference between the rotating cylinder and the LWC calculation based on the water flow rate is $|E_{rotCyl - WFR}| = 22.9\% \pm 21.3\%$ and is therefore the smallest among the presented LWC measurements. The linear best fit ($LWC_{rotCyl}=0.98 \cdot LWC_{WFR}$) through the data points has a coefficient of determination of $R^2=0.9066$. Taking into account an uncertainty of $\pm 10\%$ in the measurement results of the rotating cylinder, 78% of the measurement points are within the range of the expected value via water mass flow. Cober et al. (2001) compared the integrated LWC of the droplet sizing probes to the measurement results from the Rosemount icing (ice-accretion-based) detector. 90% of the data fall within the 1:1 correlation $\pm 64\%$. The large scatter of these data is similar to the measurements described here, although the comparison technique is different.

Figure 14 shows that both with increasing MVD and velocity the LWC tends to be slightly overestimated by the RCT. Ide (1999) found in his measurements a good agreement between the icing blade, the RCT, and two hot-wire-probes for small droplets (MVD < 40 µm). This outcome can be supported by the results presented in this study. When compared to the PDI, the RCT behaves in the exact opposite way: The LWC from the PDI measurements tend to decrease with increasing velocity, whereas the LWC from the RCT is increasing with velocity. This contrary behaviour of the two different measurement techniques calls rather not for a cause in the methodology of the water mass flow but causes in the individual measurement techniques.

5 Summary and Outlook

The Braunschweig Icing Wind Tunnel has been further developed to produce liquid droplets in the size range of 1 to 150 µm at LWC ranges of 0.1 and 2.5 g m⁻³. The droplets were accelerated to velocities between 10 and 40 m s⁻¹ and supercooled to temperatures between 0 and -20 °C. Measurements with the PDI show that the icing wind tunnel exhibits a good repeatability the MVD with a stability better than 3% and the LWC to better than 7%, as derived by standard variation. These boundary conditions permit very high reliability and stability appropriate to intercompare various droplet measuring techniques.

A probe intercomparison study of droplet size (PDI, FCDP, and shadowgraphy) and LWC (PDI, FCDP, and RCT) measurement systems was performed. Generally, the MVD measured with the FCDP and the shadowgraphy agreed within 15% to measurements with the PDI, which is in the range or better than previous tests in wind tunnels. By comparing the droplet size measurement techniques, it was possible to identify some measurement system-dependent sources of uncertainties. For the FCDP, the high sensitivity of the transit time filter to velocity differences of the droplets or a respective low sensitivity to larger particle sizes (>35 µm) was determined. Our results with the shadowgraphy setup also show the importance of the

upper part of the droplet size distribution, where the occurrence of larger droplets declines, but posing a huge impact on characteristic quantities such as the MVD and therefore requires a high number of sampled droplets per measurement point.

In addition, LWC measurements were compared to the LWC calculated from wind tunnel input parameters and the flow rate. Here, besides the rotating cylinder bulk phase instrument, the LWC was also derived from the PSD measured with the single particle probes, albeit with larger uncertainty. 65% (62%) of the LWC results measured with the RCT (PDI) agreed within 25% with the LWC determined based on the water mass flow. This is also a good overall agreement compared to existing tests. Several technology-dependent differences and error sources were identified for the LWC measurements. The PDI results showed a slight overestimation of the LWC with decreasing flow velocity. The FCDP results differ significantly from the water mass flow results. The RCT results showed very good agreement to the LWC results based on water mass flow, especially for small droplet sizes, concurring well with literature studies.

Based on these new results on the performance of the Braunschweig Icing Wind Tunnel for unimodal droplet distributions and related strength and shortcomings of instruments and measurement systems detecting PSDs and LWCs, future plans are to further enhance the capacity of the Braunschweig Icing Wind Tunnel's spray system to generate bimodal droplet size distributions. The characterization of cloud droplet distributions with particle sizes > 100 µm poses new challenges for droplet measurement techniques. The detection range has to be extended and the trajectory of large droplets and their sedimentation velocity has to be considered in the wind tunnel design and probe layout in order to accurately provide and measure a large particle spectrum. Existing knowledge in ice crystal icing experiments (e.g. Bansmer et al., 2018) can support these developments.

Author contribution

Inken Knop designed and carried out most of the described experiments. The FCDP measurements were designed and carried out by Valerian Hahn, supported by Inken Knop. Stephan Bansmer and Christiane Voigt supported the post processing and evaluation of the experiments, mainly conducted by Inken Knop (and Valerian Hahn for the FCDP). Inken Knop prepared the manuscript with the contributions from all co-authors.

Competing interests

The authors declare that they have no conflict of interest.

Acknowledgements. The presented work was conducted within the framework of the project Drífa -FKZ0325842A funded by the German Federal Ministry of Economic Affairs and Energy. Christiane Voigt and Valerian Hahn were funded by the European Union H2020 programme ICE GENESIS under contract number 824310 and by the DFG within SPP2115 PROM under contract number VO1504/5-1. The PDI measurements were strongly supported by Dr. Thomas Brämer and David Apel from LaVision GmbH, Göttingen, Germany. The authors further express their thanks to Biagio Esposito (CIRA) and Will Bachalo (Artium) for their help in interpreting the PDI results and Stephan Sattler (TU Braunschweig) and Oliver Esselmann

(former TU Braunschweig) in conducting the experiments. Finally, the authors acknowledge the support of the Open Access Publication Funds of the Technische Universität Braunschweig.

References

550

ARP5905: Calibration and Acceptance of Icing Wind Tunnels. Available online at https://www.sae.org/standards/content/arp5905/, 2015, last access: 23 July 2019.

Bachalo, W. D.: Spray diagnostics for the twenty-first century. In *Atomization and Sprays* 10.3-5 (2000): 439-474.

Bachalo, W. D.; Houser, M. J.: Phase/Doppler Spray analyzer for simultaneous measurements of drop size and velocity
555   dstributions. In *Opt. Eng* 23 (5), 235583, https://doi.org/10.1117/12.7973341, 1984.

Bachalo, W. D.; Rudoff, R. C.; Brena de la Rosa, A.: Mass Flux Measurements of a High Number Density Spray System Using the Phase Doppler Particle Analyzer, AIAA 26th Aerospace Sciences Meeting, Reno, January 11-14, https://doi.org/10.2514/6.1988-236, 1988.

Bansmer, S. E.; Baumert, A.; Sattler, S.; Knop, I.; Leroy, D.; Schwarzenboeck, A. et al.: Design, construction and
560   commissioning of the Braunschweig Icing Wind Tunnel. In *Atmos. Meas. Tech.* 11 (6), pp. 3221–3249. https://doi.org/10.5194/amt-11-3221-2018, 2018.

Basu, S.; Agarwal, A. K.; Mukhopadhyay, A.; Patel, C. (Eds.): Droplets and Sprays. Applications for combustion and propulsion, Energy, Environment, and Sustainability, Springer, Singapore, 2018.

Battisti, L.: Wind turbines in cold climates. Icing impacts and mitigation systems, Green energy and technology, Springer
565   International Publishing, Switzerland, 2015.

Baumgardner, D.; Abel, S. J.; Axisa, D.; Cotton, R.; Crosier, J.; Field, P. et al.: Cloud Ice Properties - In Situ Measurement Challenges. In *Meteorological Monographs* 58, p. 9.1. https://doi.org/10.1175/AMSMONOGRAPHS-D-16-0011.1, 2017

Baumgardner, D.: An Analysis and Comparison of Five Water Droplet Measuring Instruments. In *J. Climate Appl. Meteor.* 22 (5), pp. 891–910, https://doi.org/10.1175/1520-0450(1983)022<0891:AAACOF>2.0.CO;2, 1983.

570   Bossard, J. A.; Peck, R. E.: Droplet size distribution effects in spray combustion, *Symposium (International) on Combustion* 26 (1), pp. 1671–1677. https://doi.org/10.1016/S0082-0784(96)80391-2, 1996.

Braga, R. C., Rosenfeld, D., Weigel, R., Jurkat, T., Andreae, M. O., Wendisch, M., Pöhlker, M. L., Klimach, T., Pöschl, U., Pöhlker, C., Voigt, C., Mahnke, C., Borrmann, S., Albrecht, R. I., Molleker, S., Vila, D. A., Machado, L. A. T., and Artaxo, P.: Comparing parameterized versus measured microphysical properties of tropical convective cloud bases during the
575   ACRIDICON–CHUVA campaign, In *Atmos. Chem. Phys.*, 17, 7365-7386, https://doi.org/10.5194/acp-17-7365-2017, 2017.

Braga, R. C., Rosenfeld, D., Weigel, R., Jurkat, T., Andreae, M. O., Wendisch, M., Pöschl, U., Voigt, C., Mahnke, C., Borrmann, S., Albrecht, R. I., Molleker, S., Vila, D. A., Machado, L. A. T., and Grulich, L.: Further evidence for CCN aerosol concentrations determining the height of warm rain and ice initiation in convective clouds over the Amazon basin, Atmos. Chem. Phys., 17, 14433-14456, https://doi.org/10.5194/acp-17-14433-2017, 2017b.

580   Brenguier, J.-L.; Bourrianne, T.; Coelho, A. A.; Isbert, J.; Peytavi, R.; Trevarin, D.; Weschler, P.: Improvements of Droplet Size Distribution Measurements with the Fast-FSSP (Forward Scattering Spectrometer Probe). In *J. Atmos. Oceanic Technol.* 15 (5), pp. 1077–1090. https://doi.org/10.1175/1520-0426(1998)015<1077:IODSDM>2.0.CO;2., 1998.

Cecchini, M. A., Machado, L. A. T., Andreae, M. O., Martin, S. T., Albrecht, R. I., Artaxo, P., Barbosa, H. M. J., Borrmann, S., Fütterer, D., Jurkat, T., Mahnke, C., Minikin, A., Molleker, S., Pöhlker, M. L., Pöschl, U., Rosenfeld, D., Voigt, C.,
585   Wenzierl, B., and Wendisch, M.: Sensitivities of Amazonian clouds to aerosols and updraft speed, Atmos. Chem. Phys., 17, 10037-10050, https://doi.org/10.5194/acp-17-10037-2017, 2017.

Chuang, P. Y.; Saw, E. W.; Small, J. D.; Shaw, R. A.; Sipperley, C. M.; Payne, G. A.; Bachalo, W. D.: Airborne Phase Doppler Interferometry for Cloud Microphysical Measurements. In *Aerosol Science and Technology* 42 (8), pp. 685–703. https://doi.org/10.1080/02786820802232956, 2008.

590   Cober, S. G.; Isaac, G. A.: Characterization of Aircraft Icing Environments with Supercooled Large Drops for Application to Commercial Aircraft Certification. In *J. Appl. Meteor. Climatol.* 51 (2), pp. 265–284. https://doi.org/10.1175/JAMC-D-11-022.1, 2001.

Cossali, E.; Hardalupas, Y.: Comparison between laser diffraction and phase Doppler velocimeter techniques in high turbidity, small diameter sprays. In *Experiments in Fluids* 13 (6), pp. 414–422. https://doi.org/10.1007/BF00223249, 1992.

595   Dodge, L. G.: Comparison of performance of drop-sizing instruments. In *Applied optics* 26 (7), pp. 1328–1341. https://doi.org/10.1364/AO.26.001328, 1987.

EASA: Certification Specifications and Acceptable Means of Compliance for Large Aeroplanes. CS-25, revised 18. Available online at https://www.easa.europa.eu/sites/default/files/dfu/CS-25%20Amendment%2018_0.pdf, 2016, last access: 1 July 2019.

600   Faber, S.; French, J. R.; Jackson, R.: Laboratory and in-flight evaluation of measurement uncertainties from a commercial Cloud Droplet Probe (CDP). In *Atmos. Meas. Tech.* 11 (6), pp. 3645–3659. https://doi.org/10.5194/amt-11-3645-2018, 2018.

Fansler, T. D.; Parrish, S. E.: Spray measurement technology: A review. In *Meas. Sci. Technol.* 26 (1), p. 12002. https://doi.org/10.1088/0957-0233/26/1/012002, 2015.

Farzaneh, M.(Ed.): Atmospheric Icing of Power Networks. Dordrecht: Springer, Netherlands, 2008.

605   Flamant, C., P. Knippertz, A.H. Fink, A. Akpo, B. Brooks, C.J. Chiu, H. Coe, S. Danuor, M. Evans, O. Jegede, N. Kalthoff, A. Konaré, C. Liousse, F. Lohou, C. Mari, H. Schlager, A. Schwarzenboeck, B. Adler, L. Amekudzi, J. Aryee, M. Ayoola, A.M. Batenburg, G. Bessardon, S. Borrmann, J. Brito, K. Bower, F. Burnet, V. Catoire, A. Colomb, C. Denjean, K. Fosu-Amankwah, P.G. Hill, J. Lee, M. Lothon, M. Maranan, J. Marsham, R. Meynadier, J. Ngamini, P. Rosenberg, D. Sauer, V. Smith, G. Stratmann, J.W. Taylor, C. Voigt, and V. Yoboué, 2018: The Dynamics–Aerosol–Chemistry–Cloud Interactions
610   in West Africa Field Campaign: Overview and Research Highlights, *Bull. Amer. Meteor. Soc.,* 99, 83–104, https://doi.org/10.1175/BAMS-D-16-0256.1, 2018.

Gerber, H.; Arends, B. G.; Ackerman, A. S.: New microphysics sensor for aircraft use. In *Atmospheric Research* 31 (4), pp. 235–252. https://doi.org/10.1016/0169-8095(94)90001-9, 1994.

Gurganus, C., and P. Lawson, Laboratory and Flight Tests of 2D Imaging Probes: Toward a Better Understanding of
615   Instrument Performance and the Impact on Archived Data, 2018: *J. Atmos. Ocean Technol.*, https://doi.org/10.1175/JTECH-D-17-0202.

Ide, R. F.: Comparison of Liquid Water Content Measurement Techniques in an Icing Wind Tunnel, NASA/TM - 1999-209643, 1999.

Jackson, T. A.; Samuelsen, G. S.: Droplet sizing interferometry: a comparison of the visibility and phase/Doppler
620   techniques. In *Applied optics* 26 (11), pp. 2137–2143. https://doi.org/10.1364/AO.26.002137, 1987.

Jones, K. F.: The density of natural ice accretions related to nondimensional icing parameters. In *Q.J Royal Met. Soc.* 116 (492), pp. 477–496. https://doi.org/10.1002/qj.49711649212, 1990.

Kapulla, R. Trautmann, M.; Güntay, S.; Dehbi, A.; Suckow, D.: Comparison between phase-Doppler anemometry and shadowgraphy systems with respect to solid-particle size distribution measurements. Edited by D. Dopheide, H. Müller, V.
625   Strunck, B. Ruck, A. Leder. GALA e.V. Deutsche Gesellschaft für Laser-Anemometrie. Braunschweig (Lasermethoden in der Strömungsmesstechnik, 13), 2006.

Kapulla, Ralf; Trautmann, Mathias; Hernandez Sanchez, Alicia; Calvo Zaragoza, Salvador; Hofstetter, Sarah; Häfeli, Christoph et al.: Droplet size distribution measurements using phase-Doppler anemometry and shadowgraphy: Quantitative

comparison, GALA e.V. Deutsche Gesellschaft für Laser-Anemometrie. Rostock (Lasermethoden in der Strömungsmesstechnik, 15), 2007.

Kaufmann, S., C. Voigt, P. Jeßberger, T. Jurkat, H. Schlager, A. Schwarzenboeck, M. Klingebiel, and T. Thornberry: In situ measurements of ice saturation in young contrails, Geophys. Res. Lett., 41, https://doi.org/10.1002/2013GL058276, 2014.

Kim, K. S.; Kim, S.-S.: Drop Sizing and depth-of-field correction in TV imaging. In *Atomiz Spr* 4 (1), pp. 65–78. https://doi.org/10.1615/AtomizSpr.v4.i1.30, 1994.

Kleine, J., C. Voigt, D. Sauer, H. Schlager, M. Scheibe, S. Kaufmann, T. Jurkat-Witschas, B. Kärcher, B. Anderson: In situ observations of ice particle losses in a young persistent contrail, Geophs. Res. Lett., https://doi.org/10.1029/2018GL079390, 2018.

Kreeger, R. E.; Sankar, L.; Narducci, R.; Kunz, R.: Progress in Rotorcraft Icing Computational Tool Development. SAE Technical Paper 2015-01-2088, 2015.

Lance, S.; Brock, C. A.; Rogers, D.; Gordon, J. A.: Water droplet calibration of the Cloud Droplet Probe (CDP) and in-flight performance in liquid, ice and mixed-phase clouds during ARCPAC. In *Atmos. Meas. Tech.* 3 (6), pp. 1683–1706. https://doi.org/10.5194/amt-3-1683-2010, 2010.

Langmuir, I.; Blodgett, K.B.: The collected works of Irving Langmuir, Volume 10 - Atmospheric phenomena, chap. A Mathematical Investigation of Water Droplet Trajectories., 335-393, Pergamon press, 1961.

Lawson, R. P., C. Gurganus, S. Woods, and R. Bruintjes, Aircraft Observations of Cumulus Microphysics Ranging from the Tropics to Midlatitudes: Implications for "New" Secondary Ice Process: *J. Atmos. Sci.*, 74, 2899-2920, 2017.

Lefebvre, A. H.; McDonell, V. G.: Atomization and sprays. Second Edition. Boca Raton, London, New York: CRC Press. 2017.

Linne, M.: Imaging in the optically dense regions of a spray: A review of developing techniques. In *Progress in Energy and Combustion Science* 39 (5), pp. 403–440. https://doi.org/10.1016/j.pecs.2013.06.001, 2013.

Liu, H.-F.; Gong, X.; Li, W.-F.; Wang, F.-C.; Yu, Z.-H. Prediction of droplet size distribution in sprays of prefilming air-blast atomizers. In *Chemical Engineering Science 61* (2006), pp. 1741-1747. https://doi.org/10.1016/j.ces.2005.10.012, 2005.

Ludlam, F. H.: The heat economy of a rimed cylinder. In *Q.J Royal Met. Soc.* 77 (334), pp. 663–666. https://doi.org/10.1002/qj.49707733410, 1951.

Macklin, W. C.: The density and structure of ice formed by accretion. In *Q.J Royal Met. Soc.* 88 (375), pp. 30–50. https://doi.org/10.1002/qj.49708837504, 1962.

McDonell, V. G.; Samuelsen, G. S.: Sensitivity Assessment of a Phase-Doppler Interferometer to User-Controlled Settings. In E. D. Hirleman, W. D. Bachalo, P. G. Felton (Eds.): Liquid Particle Size Measurement Techniques: 2nd Volume. 100 Barr Harbor Drive, PO Box C700, West Conshohocken, PA 19428-2959: ASTM International, pp. 170-170-20, 1990.

McDonell, V. G.; Samuelsen, G. S.: Intra- and Interlaboratory Experiments to Assess Performance of Phase Doppler Interferometry. In Kenneth K. Kuo (Ed.): Recent Advances in Spray Combustion: Spray Atomization and Drop Burning Phenomena. Washington DC: American Institute of Aeronautics and Astronautics. 1996.

McDonell, V. G.; Samuelsen, G. S.; Wang, M. R.; Hong, C. H.; Lai, W. H.: Interlaboratory comparison of phase Doppler measurements in a research simplex atomizer spray. In *Journal of Propulsion and Power* 10 (3), pp. 402–409. https://doi.org/10.2514/3.23749, 1994.

McFarquhar, G. M.; Um, J.; Freer, M.; Baumgardner, D.; Kok, G. L.; Mace, G.: Importance of small ice crystals to cirrus properties. Observations from the Tropical Warm Pool International Cloud Experiment (TWP-ICE). In *Geophys. Res. Lett.* 34 (13), pp. n/a-n/a. https://doi.org/10.1029/2007GL029865, 2007.

670   Olsen, W.; Takeuchi, D.; Adams, K.: Experimental comparison of icing cloud instruments. AIAA-83-0026. Aerospace Science Converence. Reno, 1983.

Poots, G.; Gent, R. W.; Dart, N. P.; Cansdale, J. T.: Aircraft icing. In *Philosophical Transactions of the Royal Society of London. Series A: Mathematical, Physical and Engineering Sciences* 358 (1776), pp. 2873–2911. https://doi.org/10.1098/rsta.2000.0689, 2000.

675   ASTM E799-03, Practice for Determining Data Criteria and Processing for Liquid Drop Size Analysis, 2015.

Rudoff, R. C.; Bachalo, E. J.; Bachalo, W. D.; Oldenburg, J. R.: Liquid water content measurements using the Phase Doppler Particle Analyzer in the NASA Lewis Icing Research Tunnel. 31st ed. AIAA. Reno, Aerospace Sciences Meeting & Exhibit, 1993.

Rydblom, S.; Thornberg, B.: Liquid Water Content and Droplet Sizing Shadowgraph Measuring System for Wind Turbine
680   Icing Detection. In *IEEE Sensors J.* 16 (8), pp. 2714–2725. https://doi.org/10.1109/JSEN.2016.2518653, 2016.

Rydblom, S.; Thornberg, B.; Olsson, E.: Field Study of LWC and MVD Using the Droplet Imaging Instrument. In *IEEE Trans. Instrum. Meas.* 68 (2), pp. 614–622. https://doi.org/10.1109/TIM.2018.2843599, 2019.

Snyder, H. E.; Senser, D. W.; Lefebvre, A. H.; Coutinho, R. S.: Drop size measurements in electrostatic paint sprays. In *IEEE Trans. on Ind. Applicat.* 25 (4), pp. 720–727. https://doi.org/10.1109/28.31253, 1989.

685   Stallabrass, J.R.: An Appraisal of the Single Rotating Cylinder Method of Liquid Water Content Measurement. In National Research Council of Canada Low Temperature Laboratory, Report LTR-LT-92, 1978.

Taylor, J. W., Haslett, S. L., Bower, K., Flynn, M., Crawford, I., Dorsey, J., Choularton, T., Connolly, P. J., Hahn, V., Voigt, C., Sauer, D., Dupuy, R., Brito, J., Schwarzenboeck, A., Bourriane, T., Denjean, C., Rosenberg, P., Flamant, C., Lee, J. D., Vaughan, A. R., Hill, P. G., Brooks, B., Catoire, V., Knippertz, P., and Coe, H.: Aerosol influences on low-level clouds in the
690   West African monsoon, Atmos. Chem. Phys., 19, 8503-8522, https://doi.org/10.5194/acp-19-8503-2019, 2019.

Thornberry, T., Rollins, A., Avery, M., Woods, S., Lawson, P., Bui, P., Gao, R.-S., Ice water content-extinction relationships and effective diameter for TTL cirrus derived from in situ measurements during ATTREX 2014, 2017: *J. Geophys. Res. Atmos.*, https://doi.org/10.1002/2016JD025948.

Tropea, C.: Optical Particle Characterization in Flows. In *Annu. Rev. Fluid Mech*. 43 (1), pp. 399–426.
695   https://doi.org/10.1146/annurev-fluid-122109-160721, 2011.

Tuck, C. R.; Butler Ellis, M.C.; Miller, P.C.H: Techniques for measurement of droplet size and velocity distributions in agricultural sprays. In *Crop Protection* 16 (7), pp. 619–628. https://doi.org/10.1016/S0261-2194(97)00053-7, 1997.

Voigt, C., U. Schumann, P. Jessberger, T. Jurkat, A. Petzold, J.-F- Gayet, M. Krämer, T. Thornberry, D. Fahey: Extinction and optical depth of contrails, *Geophys. Res. Lett.*, 38, L11806, https://doi.org/10.1029/2011GL047189, 2011.

700   Voigt, C; Schumann, U; Minikin, A. et al.: The Airborne Experiment on Natural Cirrus and Contrail Cirrus with the High Altitude Long-Range Research Aircraft Halo. Bulletin on the American Meteorological Society, https://doi.org/10.1175/BAMS-D-15-00213.1, 2017.

Wendisch, M.; Pöschl, U.;, Meinrat O. A. et al.,ACRIDICON-CHUVA Campaign Studying Tropical Deep Convective Clouds and Precipitation over Amazonia Using the New German Research Aircraft HALO, Bulletin on the American
705   Meteorological Society, https://doi.org/10.1175/BAMS-D-14-00255.1, 2016.

Widmann, J. F.; Presser; C.; Leigh, S. D.: Improving phase Doppler volume flux measurements in low data rate applications. In *Measurement Science and Technology* 12 (8), p. 1180, 2001.

Woods, S., P. Lawson, E. Jensen, T. Thornberry, A. Rollins, P. Bui, L. Pfister, M. Avery, Microphysical Properties of Tropical Tropopause Layer Cirrus, 2018: *J. Geophys. Res. Atmos.*, https://doi.org/10.1029/2017JD028068

710 Zhu, J. Y.; Rudoff, R. C.; Bachalo, E. J.; Bachalo, W. D.: Number Density and Mass Flux Measurements Using the Phase Doppler Particle Analyzer in Reacting and Non-Reacting Swirling Flows. 31st AIAA. Reno, 1992.
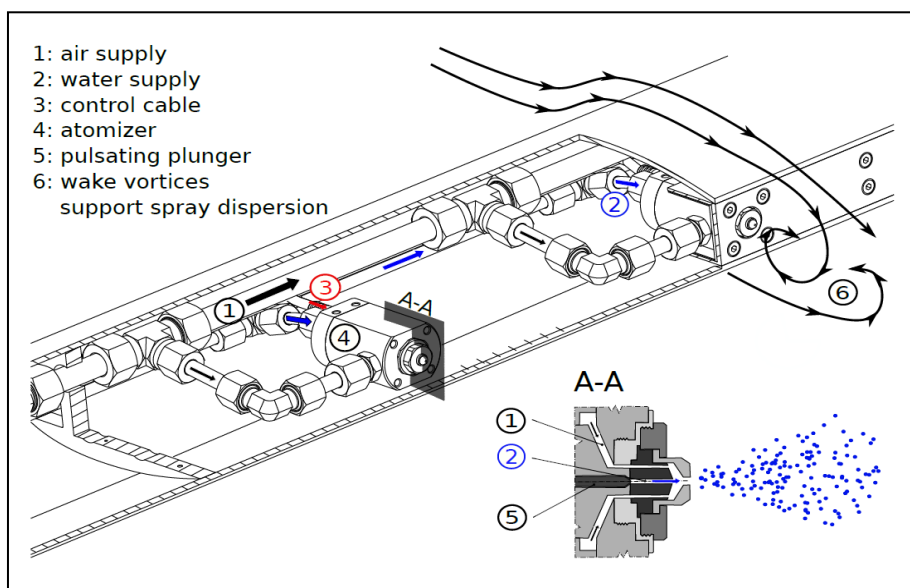
Figure 1: Spray system in the Braunschweig Icing Wind Tunnel (Bansmer et al. 2018).
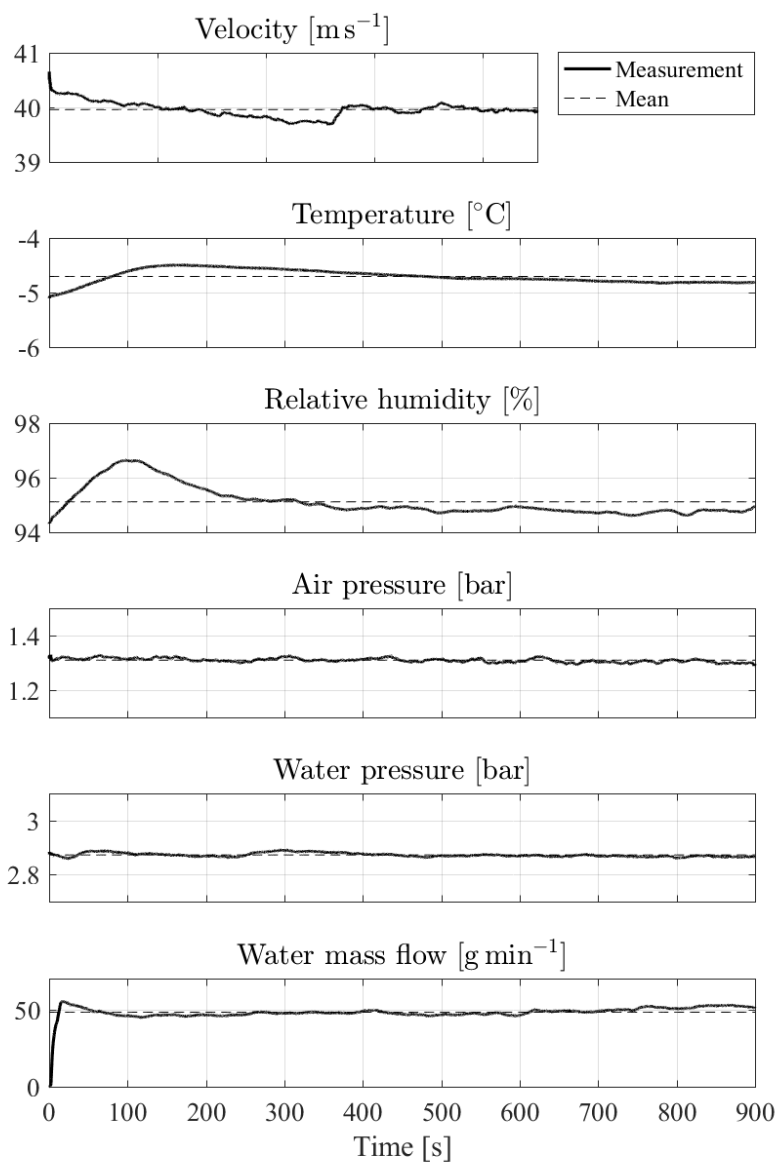
Figure 2: Exemplary stability of the wind tunnel conditions over 15 minutes test duration.
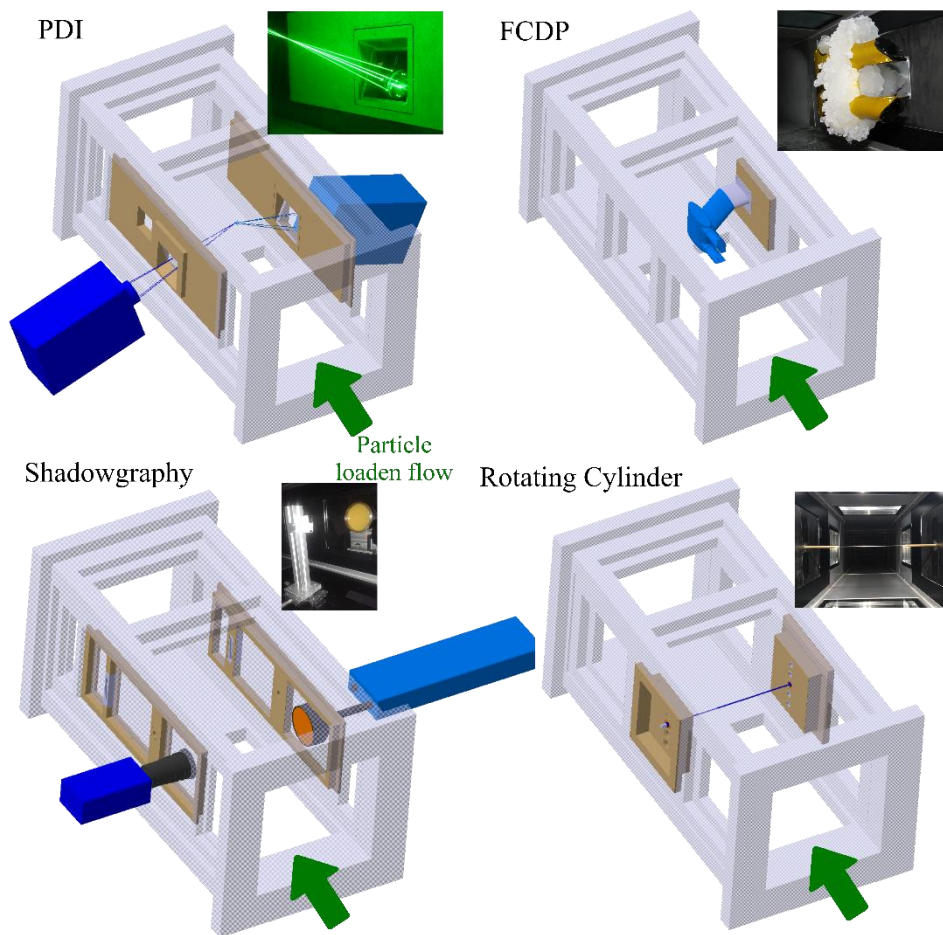
Figure 3: Measurement setups in the Braunschweig Icing Wind Tunnel.
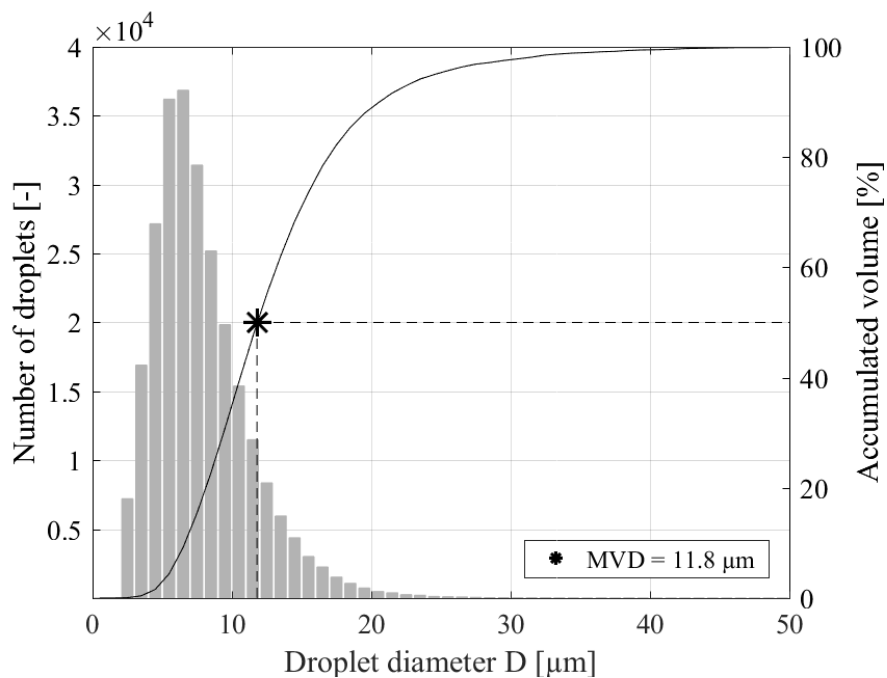
Figure 4: Droplet diameter histogram and cumulative volume curve at 20 m s⁻¹ (PDI Run 18/04/19 17:19).
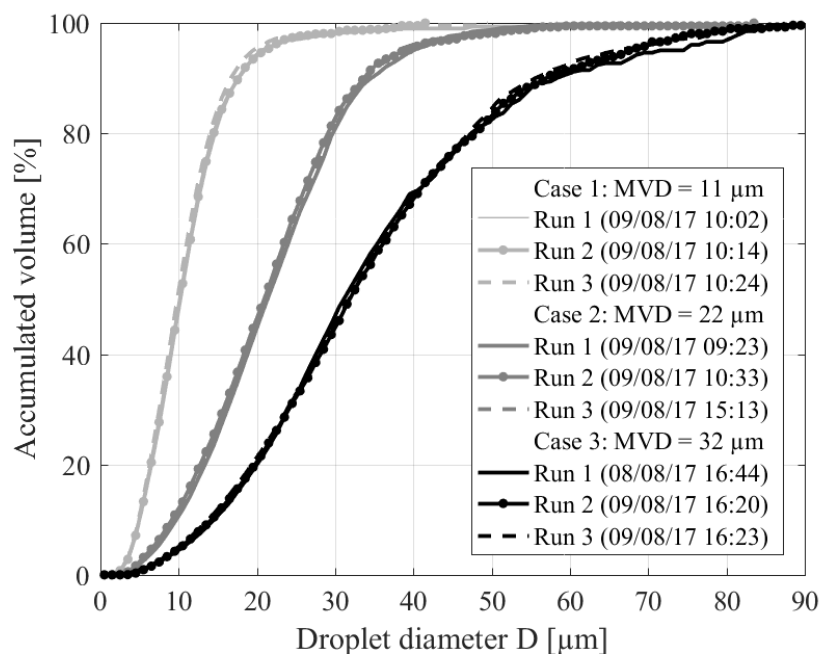
725   **Figure 5: Wind tunnel repeatability shown with PDI measurements at 40 m s⁻¹.**
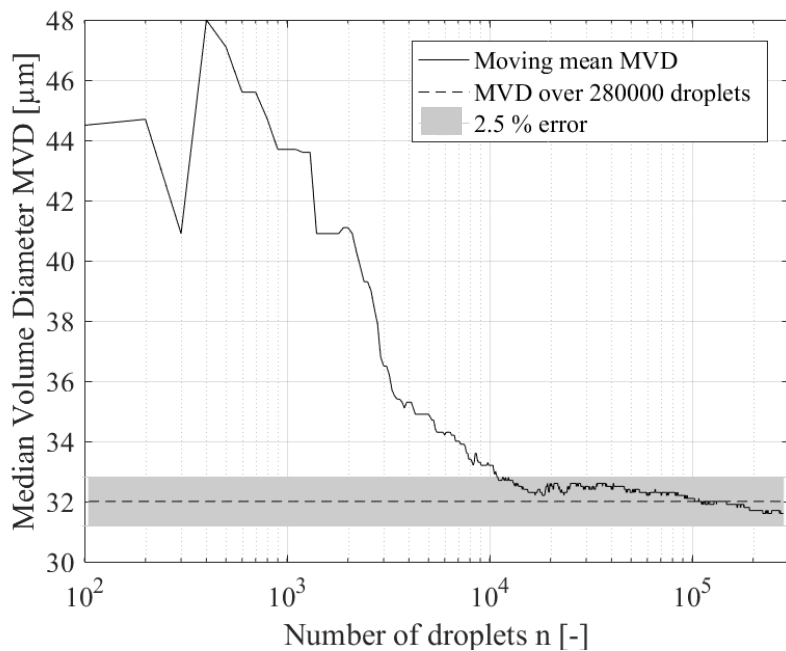
Figure 6: Convergence of MVD over number of droplets at 40 m s⁻¹ (PDI Run 09/08/17 17:59).
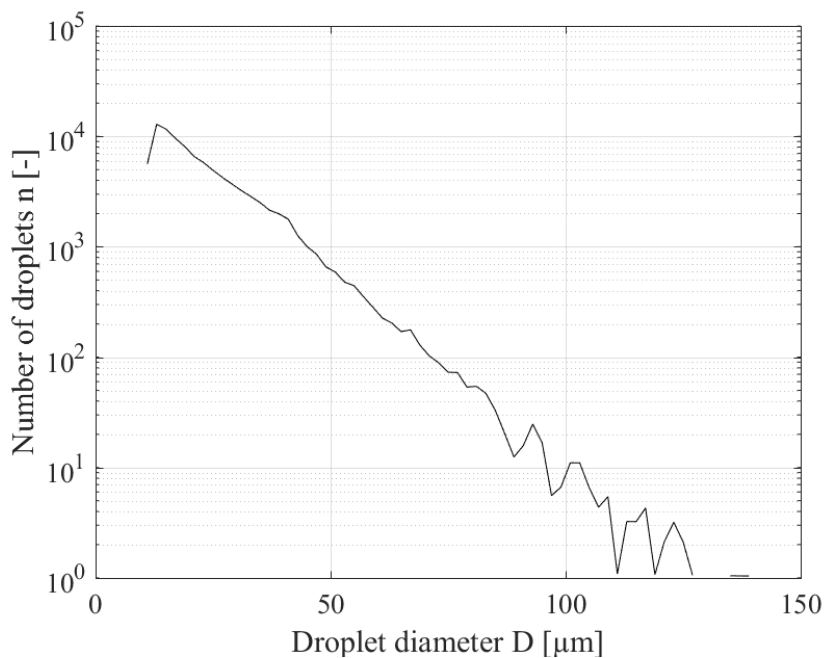
730   **Figure 7: Number of droplets over diameter (PDI Run 18/04/19 18:25), total number of counts >95000.**
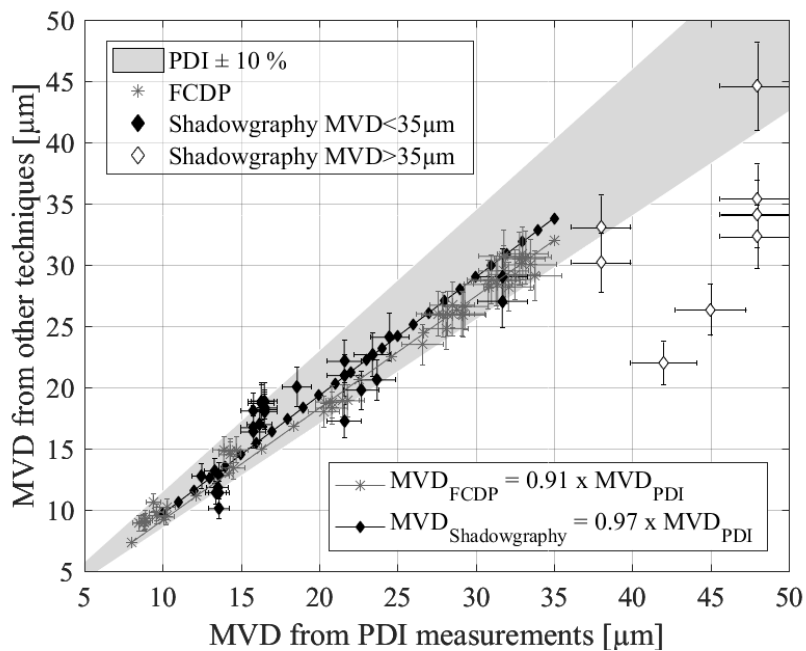
Figure 8: Intercomparison of MVD measured with the PDI, the FCDP and the shadowgraphy.
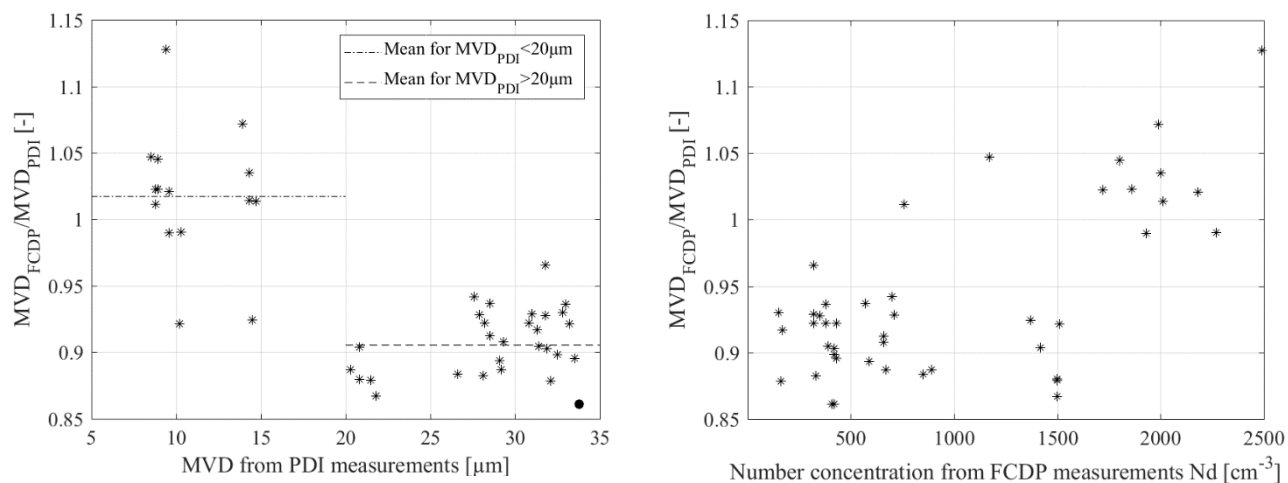
Figure 9: Effect of MVD on droplet size measurements from the FCDP (left) and effect of number concentration (right).

735
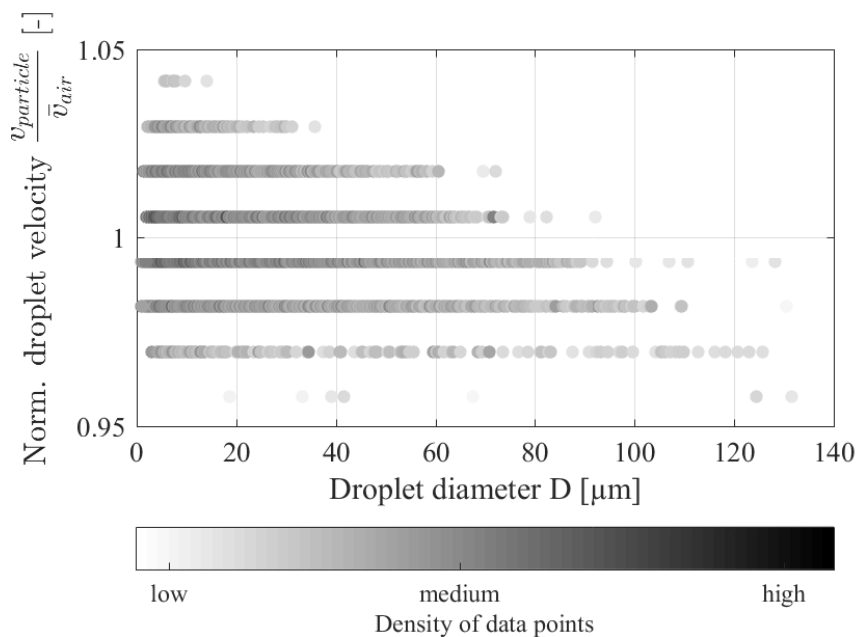
Figure 10: Droplet velocity over diameter (PDI Run 08/08/17 16:25).
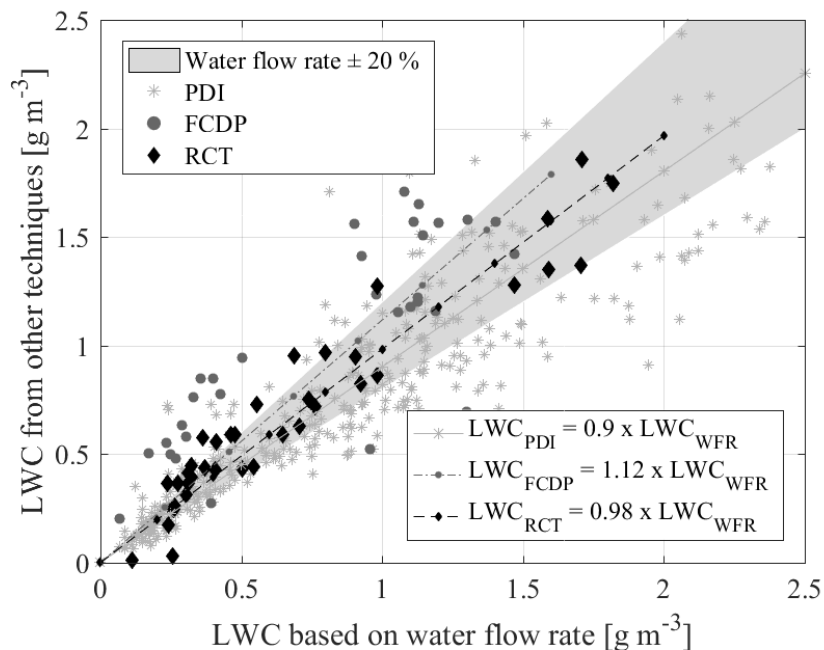
740 **Figure 11: Intercompatrison of LWC based on the water flow rate and measured with the PDI, the FCDP and the RCT.**
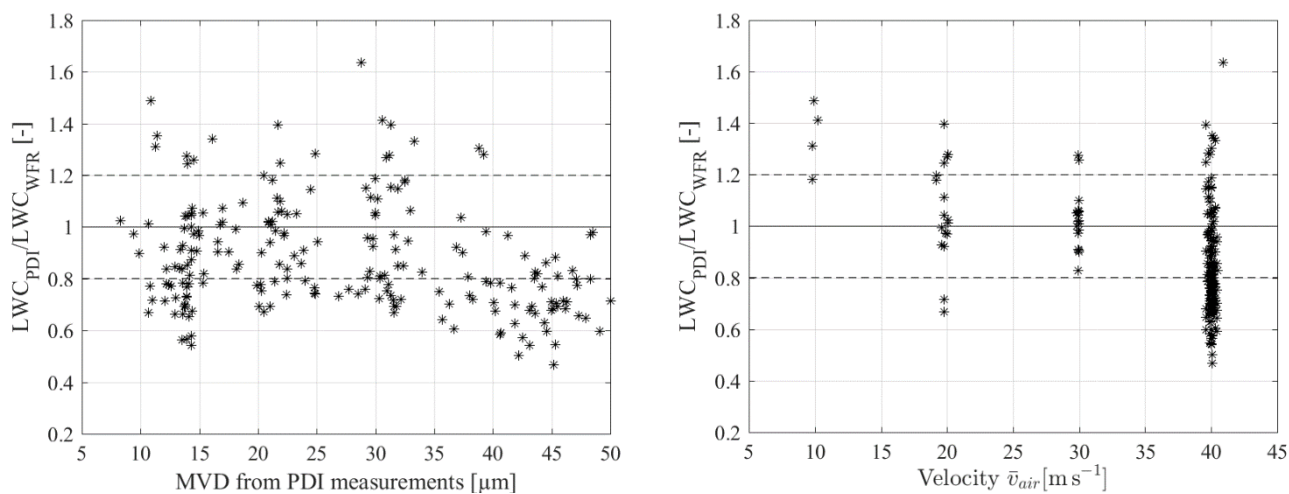
Figure 12: Effect of MVD on LWC measurements from the PDI (left) and effect of air velocity (right).
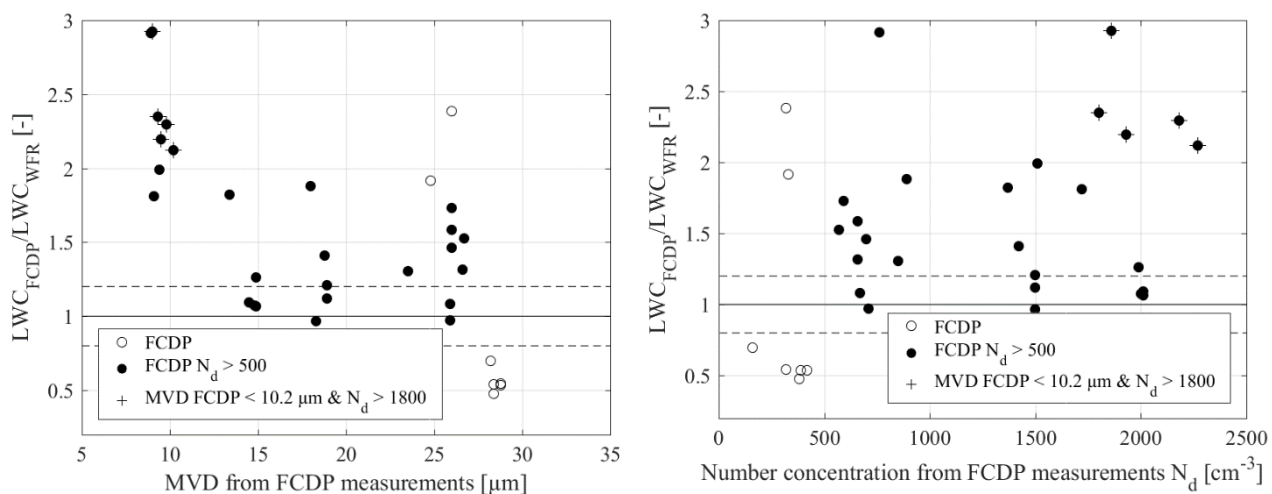
745   **Figure 13: Effect of MVD on LWC measurements from the FCDP (left) and effect of number concentration (right).**
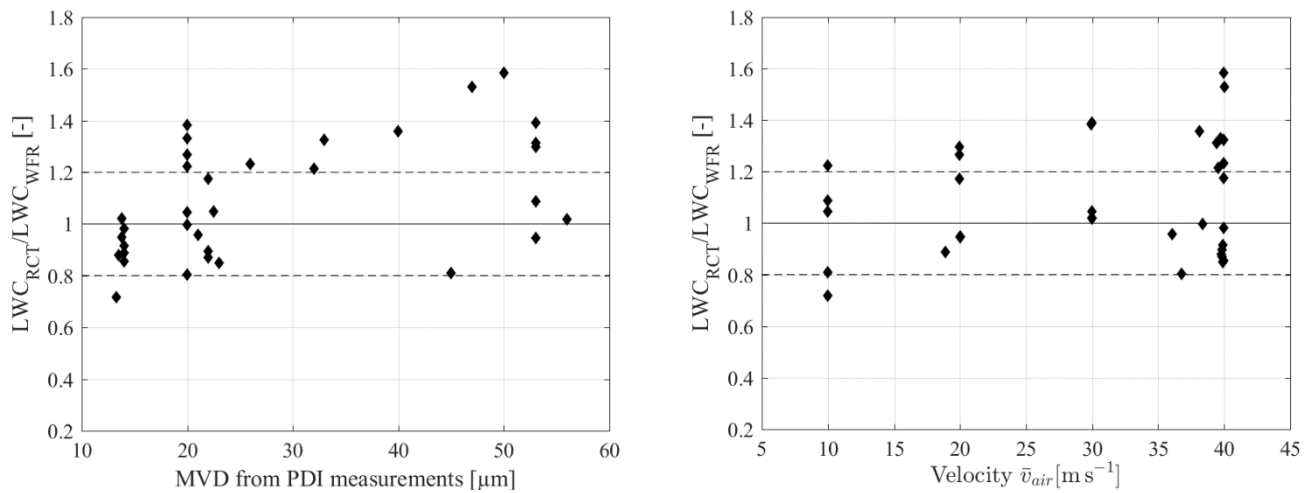
Figure 14: Effect of MVD on LWC measurements from the RCT (left) and effect of air velocity (right).

750 **Table 1: Characteristic numbers of PDI setup**

Transmitter		Receiver	
Wave-length	532 nm	Focal length	500mm
Focal length	350 mm/ 500 mm	Collection Angle	40 ° ± 1°
Beam Separation	59.4 mm	Slit Aperture	100 µm
Beam diameter	2.33 mm	PMT Gain	300-500 V
Expander Factor	1	Domination scattering order	refraction
Frequency Shift	40 MHz		
Fringe Spacing	3.1 µm/ 4.5 µm	Static Range	0.9 - 134.4 µm 1.3 - 191.7 µm (2.6 -571.2 µm)
Beam Waist at probe volume	101.7 µm/ 145.4 µm		

Table 2: Characteristic numbers of FCDP setup

Wavelength	785 nm	DOF crit.	0.9
Domination scattering order	Forward Scattering	Bin number	21
Collection Angle	4-12 °	Bin widths	1.5-4 µm
Beam width diameter	0.08 cm	Size Range	1.5-50 µm
Qualifier Slit width	0.009 cm		

755

Table 3: Characteristic numbers of shadowgraphy setup

Laser	Pulsed Nd-YAG laser	Camera	PCO Sensicam 12bit
Energy	1200 mJ	Resolution	1376 x 1070 px
Pulse duration	4 ns	Scale	1.9 x 1.9 µm ≙ 1 Pixel

760 **Table 4: Coefficient of variation of the wind tunnel conditions for measurements with the different measurement techniques**

σ	MVD	DV0.1	DV0.9	DV0.99	LWC
PDI	5 %	7 %	7 %	14 %	20 %
FCDP	7 %	10 %	6 %	-	17 %
Shadowgraphy	8 %	9 %	8 %	-	-
Rotating cylinder	-	-	-	-	< 10 %
Water mass flow	-	-	-	-	7 %